Australian Journal of Basic and Applied Sciences, 9(27) August 2015, Pages: 327-339

ISSN:1991-8178

Australian Journal of Basic and Applied Sciences

Journal home page: www.ajbasweb.com

Effect of Indium Concentration on The Main Detection Parameters of In_xSe_{1-x} Photodetector

Bushra A.Hasan and Iyat M.Abdulrazzaq

University of Baghdad, College of science, Physics Department, Baghdad, Iraq

ARTICLE INFO

Article history:
Received 23 June 2015
Accepted 25 August 2015
Available online 2 September 2015

Keywords:
In_xSe_{1-x} thin films, thermal evaporation technique, XRD, SEM, EDAX

ABSTRACT

A polycrystalline In_xSe_{1-x} alloys with various In content (10, 20,30, and 40)% has been prepared successfully, the structure and composition of alloys are determined by X-ray diffraction (XRD), atomic force microscopy (AFM) and X-ray fluorescence (EDX) respectively. The X-ray diffraction studiy shows that the structure of the prepared thin films samples was semi crystalline for low indium content and increases of thickness increases degree of crystallinity while amorphous for high indium content. From AFM and EDAX studies, the average grain size increases with increase and thickness and indium content up x=0.1 and then decreases while roughness showed opposite manner . The concentration of In and Se content for alloys was determined, and the results showed high accuracy and nearly close to the theoretical values. Films of In_xSe_{1-x} of different thickness (300, 500, and 700nm) have been deposited on glass and n-Si substrates by thermal evaporation method at room temperature. The optical study of In_xSe_{1-x} thin films is carried out in the wavelength range 300-1100 nm at room temperature. The optical measurement showed that In_xSe_{1-x} films with direct and indirect energy gap(E_g), which changes with increasing thickness and In content. The photoconductive properties were measured. A photoconductive detector In_xSe_{1-x} film has been fabricated by depositing In_xSe_{1-x} thin films on Si (n- type) substrate with (111) direction by thermal evaporation at different x content and thickness. Photoconductive, I-V have been studied. The spectral resonsivity(R_λ), quantum efficiency η,and spectral detectivity (D^*) were determined as function of wavelength, also the resistance, conductivity in dark and with illumination to infrared radiation, and relative photo response have been measured with different indium concentration. Remarkable improvements in the photoresponse were observed for the highest resistance specimen with low indium concentration at the expense of spectral detectivity values.

© 2015 AENSI Publisher All rights reserved.

To Cite This Article: Bushra A.Hasan and Iyat M.Abdulrazzaq., Effect of Indium Concentration on The Main Detection Parameters of InxSe1-x Photodetector. ***Aust. J. Basic & Appl. Sci.,*** *9(27): 327-339, 2015*

INTRODUCTION

Indium Selenide (InSe) belongs to III –VI compounds family being a layered semiconductor consisting of covalent bonded units (Se-In-In-Se) held together by Van der Walls forces and is one of the most suitable compound semiconductors for optoelectronic and photovoltaic applications (Hasegawa, Y., Y. Abe, 1982). Being a layer-type semiconductor, its two-dimensional structure and its resulting anisotropic properties are of particular interest. Literature reports indicate that InSe thin films have been prepared by a number of techniques by a number of researchers. These include the vacuum evaporation (Peršin, M., *et al*., 1970; Viswanathan, C., *et al*., 2005; Di Giulio, M., *et al*., 1987), flash evaporation (Peršin, M., *et al*., 2005), molecular beam deposition (Viswanathan, C., *et al*., 2005), electrodepositing (Gopal, S.,), sol-gel method (Mutlu, I.H., *et al*., 2007), etc. In the present study, we developed new photosensitive p- In_xSe_{1-x} /n-Si photodetectors. We report on surface morphology of In_xSe_{1-x} thin films deposited onto n-Si substrates, as well as photoelectrical properties of the obtained photodetectors .Also the optical properties of In_xSe_{1-x} thin films, prepared by thermal evaporation technique onto glass substrate, have been studied. The structural properties have been studied by using X-ray diffraction (XRD), scanning electron microscopy (SEM) and energy dispersive analysis of X-ray (EDAX).

2. Experimental:

The starting material was prepared by mixing quantities of high-purity (99.999%) indium and selenium powder shot in various atomic weight proportion 10/90, 20/80, 30/70, and 40/60. The mixture was sealed in an evacuated quartz tube at pressure 10^{-5} torr and heated at 1073 K for 10 hr in furnace and then quenched in air. In_xSe_{1-x} films have

Corresponding Author: Bushra A.Hasan, University of Baghdad, College of science, Physics Department, Baghdad Iraq.
E-mail: bushra_abhasan@yahoo.com

been deposited by thermal evaporation technique under vacuum of about 10^{-5} torr. The substrate to source distance was kept 15cm. The samples of different thicknesses were deposited under similar conditions. The thickness of the films was estimated using the weighting method which provided that the evaporation was done on half circle. In each deposition, a given quantity of material was taken in the boat of molybdenum and evaporated at the rate of 5 to10 A^0 per second. Before evaporation, the glass substrates were cleaned thoroughly using concentrated chromic acid, detergent, isopropyl alcohol and distilled water. The film thickness was measured by the Tolanasky interference method with an accuracy of ±10 nm (Tolansky, S., 1948).

X – Ray diffractogram (Rigaku Miniflex, Japan) were obtained of these samples to find out structural information and to identify the film structure qualitatively. The scanning angle (2θ)range was from 20^0 - 80^0 (CuKα line). Optical absorption was measured by UV-VIS spectrophotometer model no. Shimadzu -2450. The sample deposited on glass was placed in front of the reference beam and the spectra were collected. The conductivity σ of the samples was determined from the relation, $\sigma = ((V\ A)/(IL))^{-1}$ with A and L being the cross-sectional area and the length of the film. The dark current of In_xSe_{1-x} photoconductive films at different value of x content and thickness was measured as a function of applied voltage (0-6 Volt). The photocurrent measurement have been done by using system consists of Ultraviolet-Visible halogen source in the region (200-1000nm) and supplied with D.C power supply, monochrometer in the range 200-600nm type spectrometer model 746 from optronic Laboratories, Keithly Digital Electrometer for measuring the current. The sample of In_xSe_{1-x} films with different value of x content and thickness were connected to the electrical circuit. By increasing the incident light wavelength, the photocurrent was measured with the Keithly Digital Electrometer and the incident power on the detector was obtained by using a intensity meter. The photocurrent measurement have been done by using system consists of ultraviolet visible source with D.C power supply, monochrometer in the range 200-700nm type spectrometer model 746 from optronic Laboratories, KeithlyDigital Electrometer for measuring the current. The noise is referred to the signal generated in the detector at the absence of the radiation. The noise current is given by (Viswanathan, C., *et al*., 2005): $I^2=2q[I_P+(I_{Sat}/\beta)e^{qV/\beta k_B T}+k_BT/qR_D]\Delta F$,Where ($I_P=AGq\eta\varphi_B$), and φ_B is power density of the background. The relation between dark current and noise current is (Viswanathan, C., *et al*., 2005; Grigorov, S.N., *et al*., 2004):$I_n=(2qI_d\Delta F)^{1/2}$,Where I_d is dark current, Δ F is bandwidth. The first two terms of the above equation represent generation noise(g_r) due to the background photon flux, they represent the thermal equilibrium carriers in semiconductors and they called shot noise as result to applied external field (bias voltage). The third term represents Johnson noise and it depend on the material resistance of semiconductor. gr noise and Johnson noise are the fundamentals mechanism of photoconductive detectors.

Noise Equivalent Power (NEP) is defined as incident radiation power required to produce signal equal to the r.m.s noise voltage (S/N) or can be defined as the generated current noise divided by the spectral responsivity of the detector as in the relation: $NEP = I_n/R_\lambda$,Detectivity (D) is originally defined as reciprocal of NEP[10,11]:$D=1/NEP= R_\lambda / I_n$ and specific Detectivity (D^*) also known as normalized detectivity, is a reciprocal of the NEP, normalized to a detector area of 1 cm^2 and an electrical bandwidth of 1 Hz, with assuming that the detectivity noise varies with $A^{1/2}$and $\Delta F^{1/2}$. The (D^*) is expressed as (Rusu, G.G., 2001):
$D^*=(A\ \Delta F)^{1/2}/NEP)$ or[9,10]: $D^*= R_\lambda (a`\ \Delta F)^{1/2} / I_n$

The value of D^* is independent on the size of detector and depend on the wavelength of signal radiation and frequency at which it is modulated (Viswanathan, C., *et al*., 2005).

Quantum efficiency (η) is the ratio between number of elementary events contributing to the detector output to the number of incident photons. For photoelectric detector whose output is a current, the quantum efficiency can be computed from current responsivity (Viswanathan, C., *et al*., 2005):$\eta_{(\lambda)}=R_\lambda hc/\lambda q=1.24R_\lambda/\lambda$, the parameters from this equation depends on the wavelength. The value of η is always less than one, it increases when the value the absorption within depletion layer by increasing the reverse voltage or making a shallow junction that does not allow recombination of the carriers before collecting it in the depletion region by increasing lifetime of carriers (Krus, P.W., 1977; Samuel Lioo, Y., 1984).

RESULTS AND DISCUSSION

3.1 X-ray Diffraction (XRD) Study:

The X-ray difractograms of as deposited In_xSe_{1-x} samples with different In content and different thickness (not shown here) depicts that as-deposited $In_{10}Se_{90}$ and $In_{20}Se_{80}$ films with low thickness (t=300nm)begin to crystallize since only one small peak observed. The increase of thickness lead to well crystallization of the prepared samples films, which reflects as the increase of peaks numbers at x=700nm as well as increase the peak intensity.

The interesting result for as-deposited $In_{30}Se_{70}$films is the absent of any diffraction peak which indicate the amorphous nature of the prepared films with low thickness (i.e.t=300 and 500nm)begin to crystallize with increase of thickness to 700nm . Further increase of In concentration lead to significant result is the absent of any diffraction peak which indicate the amorphous nature of all the as -

deposited $In_{40}Se_{60}$films films , the increase of thickness lead to transform the structure from amorphous to polycrystalline. The increase of indium concentration lead to decrease the degree of crystillanity. So it can be concluded that amorphous In_xSe_{1-x} thin films become polycrystalline after structural transformation as result of increase of thickness. The similar phenomena have been investigated by other researchers (Viswanathan, C., *et al*., 2005; Grigorov, S.N., *et al., 2004;* Rusu, G.G., 2001).

3.2 Atomic Force Microscopy (AFM) and EDAX Study:

Figs. 1 show the AFM images of the In_xSe_{1-x} thin films with different In content and thickness, respectively. AFM images revealed the growth of randomly oriented, worm-like grains, which are uniformly distributed over the surface. It is obvious from table .1 that the average grain size get to increase with increasing of In content for low indium content, while the average of grain size get to decrease with further increase of indium concentration, indeed the average grain increases from 81.1 to 92.98nm when x increase from 0.1 to 0.2and then decreases to 44.87 nm for x=0.4 .The increase of average of grain size with indium concentration attributed with structure enhancement and increase degree of crystallinity, which coincides with XRD results, while the decrease of average of grain size attributed to decrease the degree of crystallinity and the tendency to amorphous rather than crystalline structure of the films with high indium content. Although there is no systematic of the variation of roughness with indium concentration, but in general the roughness exhibit to change in opposite manner with increase indium concentration, i.e. the maximum value of roughness (corresponding to minimum value of the average of grain size and visa versa. On the other hand the grain size increases with thickness for all indium concentration ,moreover the grain size increase from 81.1to 149nm and from 92.9 to 105 nm and from 47.2 to 73.8nm and from 44.87 to 80.89 nm for $In_{10}Se_{90}$,$In_{20}Se_{80}$, $In_{30}Se_{70}$, and $In_{40}Se_{60}$ when thickness increases from 300nm to 700nm respectively. The increase of grain size with thickness resulted from structural enhancement since increase of thickness lead to structure transformation from amorphous to polycrystalline, while increases of thickness lead to decrease roughness of the all the prepared In-Se binary system.

From the micrograph it is clearly seen that grain size increased with increase of In, which is clearly observed . however maximum value the grain size grain size 149.5 nm attain with indium content x=30%wt. The formation of bigger grains is due to coalescence of smaller grains. Availability of thermal energy at higher indium content is responsible for increased grain size. In contrast to that The average surface roughness were found to decrease with increase of indium and thickness. The variation of grain size and surface roughness, with thickness is indicated in Table.1. The analysis of the elemental compositions for the In_xSe_{1-x} thin films of various thicknesses were estimated by using the method of Energy Dispersive Analysis of X-ray (EDAX). The result of elemental composition by EDAX study for In_xSe_{1-x} thin films of thickness 300, 500, and 700 nm, respectively is shown in Table. 2

3.3 Optical Properties:

The transmittance of In_xSe_{1-x} thin films with different indium content and of thicknesses 300, 500, and 700nm are shown in Figs. 3.The transmittance decreases with increase of In content up x=0.2 and then increases which attributed to decrease of reflectance or the samples become more opaque with increase of In content. Also the transmittance decreases with thickness. This resells form increase of density.

Sample	thickness(nm)		
	300	500	700
$In_{10}Se_{90}$	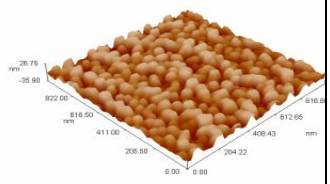	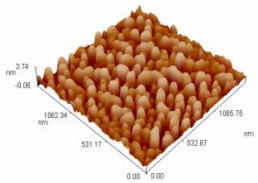	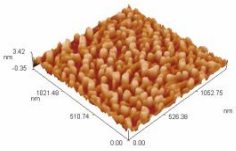
$In_{20}Se_{80}$	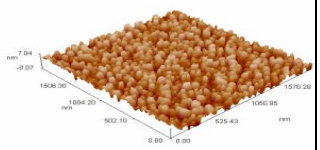	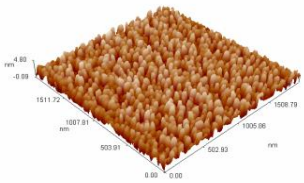	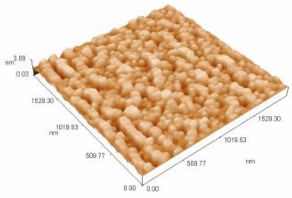
$In_{30}Se_{70}$	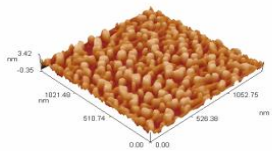	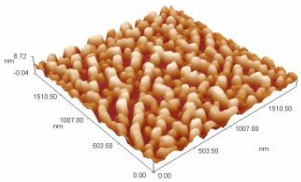	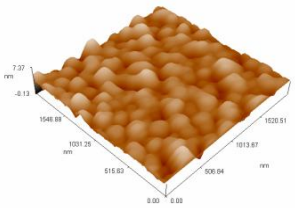
$In_{40}Se_{60}$	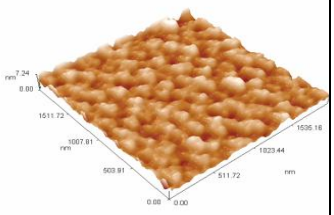	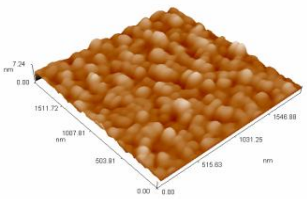	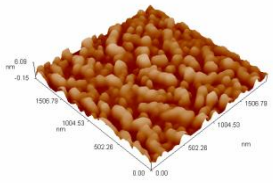

Fig.1AFM pictures for In_xSe_{1-x} thin films with different In content at different thickness.

Table 1: Average grain size and average roughness for In_xSe_{1-x} films with different In content at different thickness.

Sample	Thickness (nm)	Average grain size (nm)	Average roughness (nm)
$In_{10}Se_{90}$	300	81.1	0.608
	500	77.05	0.519
	700	149.51	0.555
$In_{20}Se_{80}$	300	92.98	0.682
	500	102.44	0.534
	700	105	0.836
$In_{30}Se_{70}$	300	47.21	2.42
	500	70.51	0.667
	700	73.85	0.507
$In_{40}Se_{60}$	300	44.87	1.02
	500	41.99	0.791
	700	80.89	0.27

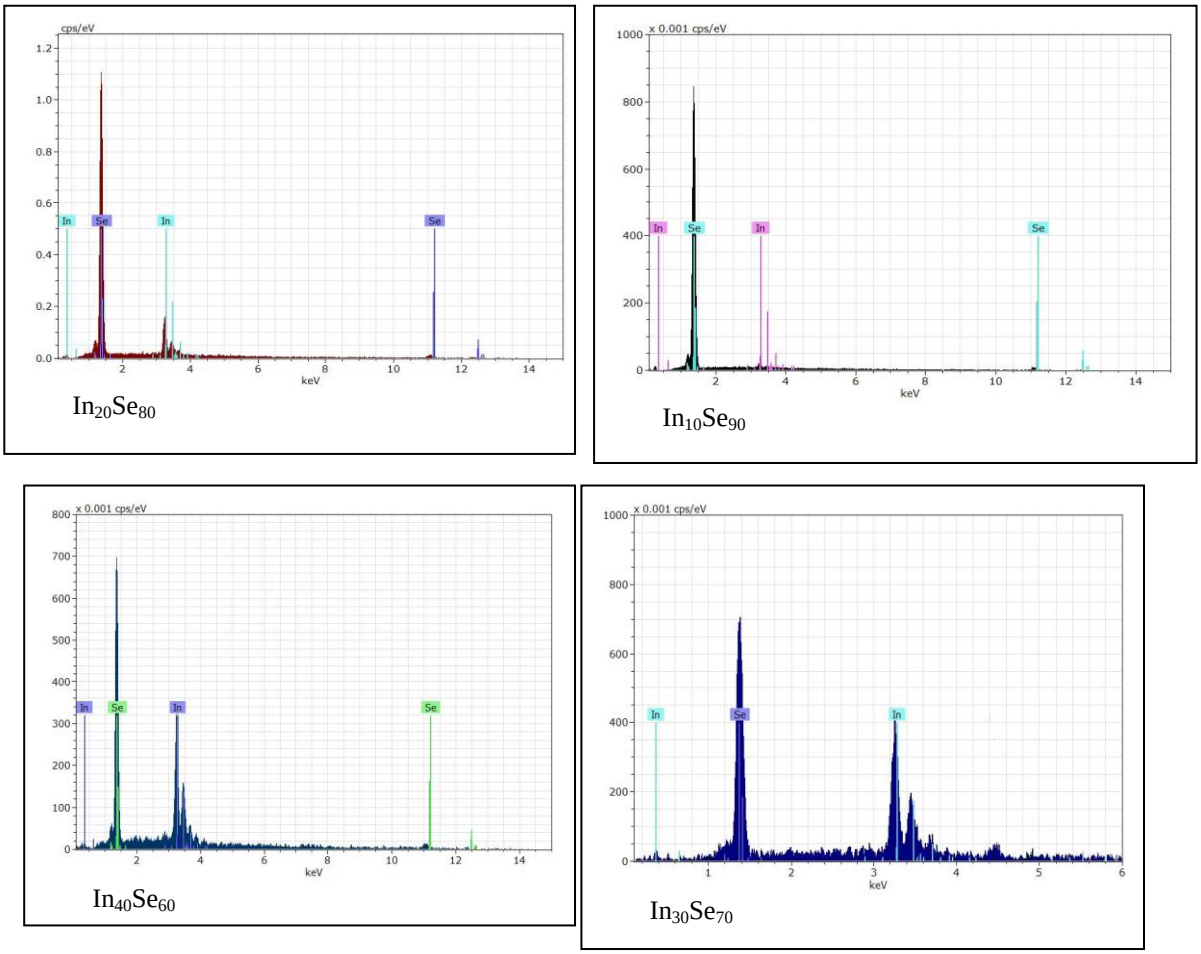

Fig. 2: EDAX patterns for In_xSe_{1-x} alloys with different In content.

Table 2: Composition analysis using (EDX) technique

Experimental concentration		Theoretical concentration		Alloy
Se	In	Se	In	
97.06	2.94	90	10	$In_{10}Se_{90}$
83.11	16.89	80	20	$In_{20}Se_{80}$
71.71	28.29	70	30	$In_{30}Se_{70}$
68.53	31.47	60	40	$In_{40}Se_{60}$

In the high absorption region, absorption coefficient (α) can be represented by the relation as Tauc (Tauc, J., 1974) and Pankove (Pankove, J.I., 1971), respectively, $(\alpha h\nu)^{1/r} = A(\alpha h\nu - Eg^{opt})$ where A is constant depending on the transition probability, Eg is the optical band gap and r is an index that characterizes the optical absorption process and is theoretically equal to 2, 1/2, 3 or 3/2 for indirect allowed (Savitskii, A.V., *et al*., 1964), direct allowed, indirect forbidden and direct forbidden transitions, respectively. The usual method for determining the value of the band gap Eg^{opt} is obtained from a graph of $(\alpha h\nu)^{1/r}$ versus photon energy hv . If an appropriate value of r is used to obtain a linear plot, the value of Eg will be given by the intercept on the hv axis. Fig. 4 and 5 show the plot of $(\alpha h\nu)^2$ vs. hν and $(\alpha h\nu)^{1/2}$ vs. hν for the In_xSe_{1-x} thin film of different thickness . The optical absorption coefficient is of the order of 10^6 cm^{-1} supporting the allowed direct band transition of the material (Viswanathan, C., *et al*., 2005; Viswanathan, C., *et al*., 2004; Qasrawi, A.F., 2007). The higher value of α in the UV region makes the material useful in forming p-n junction solar cells with other suitable thin film materials for photovoltaic applications (El-Zahed, H., *et al*., 2003). The optical band gap Eg^{opt} is determined near the absorption edge by extrapolating the straight portion of the plot of energy axis. The calculated values of direct band gap Eg^{opt} for different thickness samples vary between 2.15 to 2.05 eV and from 2.1 to1.8 eV and from 2.2 to1.85 eV and from2.3 to 1.6 eV of $In_{10}Se_{90}$ of $In_{20}Se_{80}$ of $In_{30}Se_{70}$ of $In_{40}Se_{60}$ respectively, which well agree with early reports (Viswanathan, C., *et al*., 2005; Viswanathan, C., *et al*., 2005; Viswanathan, C., *et al*., 2004). This decrease of band gap with thickness may be attributed to the presence of unstructured defects,

which increase the density of localized states in the band gap and consequently decrease the energy gap (Qasrawi, A.F., 2007).

The calculated values of direct and indirect band gap (Eg) for different thickness of In_xSe_{1-x} samples decrease with increased of indium content up x=0.2 and then increases as shown in table 3. This behavior explained on the basis of structure, since increase of indium from 10 to 20% enhanced the structure through out increases the grain size while further increase of indium content lead to phase transformation from crystalline to amorphous. It known worthy that polycrystalline material has wider energy gap than amorphous material. Also the decrease of Eg^{opt} with the increase of In content is because the addition of In causes the creation of new localized states in the band gap which result in visual decrease of Eg^{opt} values. On the other hand Eg^{opt} decrease with increase of thickness. The decrease of Eg^{opt} with the increase of thickness is explained as follows: It is well known that Eg^{opt} value of bulk material is lower than that of film sample, thus the increase of thickness causes the reduction of Eg^{opt} values since the structure will approach that of bulk material.Indirect energy gap also decreases with the increase of the thickness and show the similar behavior with increase of In content (El-Zahed, H., *et al*., 2002; Mott, N.F. and E.A. Davis, 1979; Parlak, M. and Ç. Erçelebi, 1998).

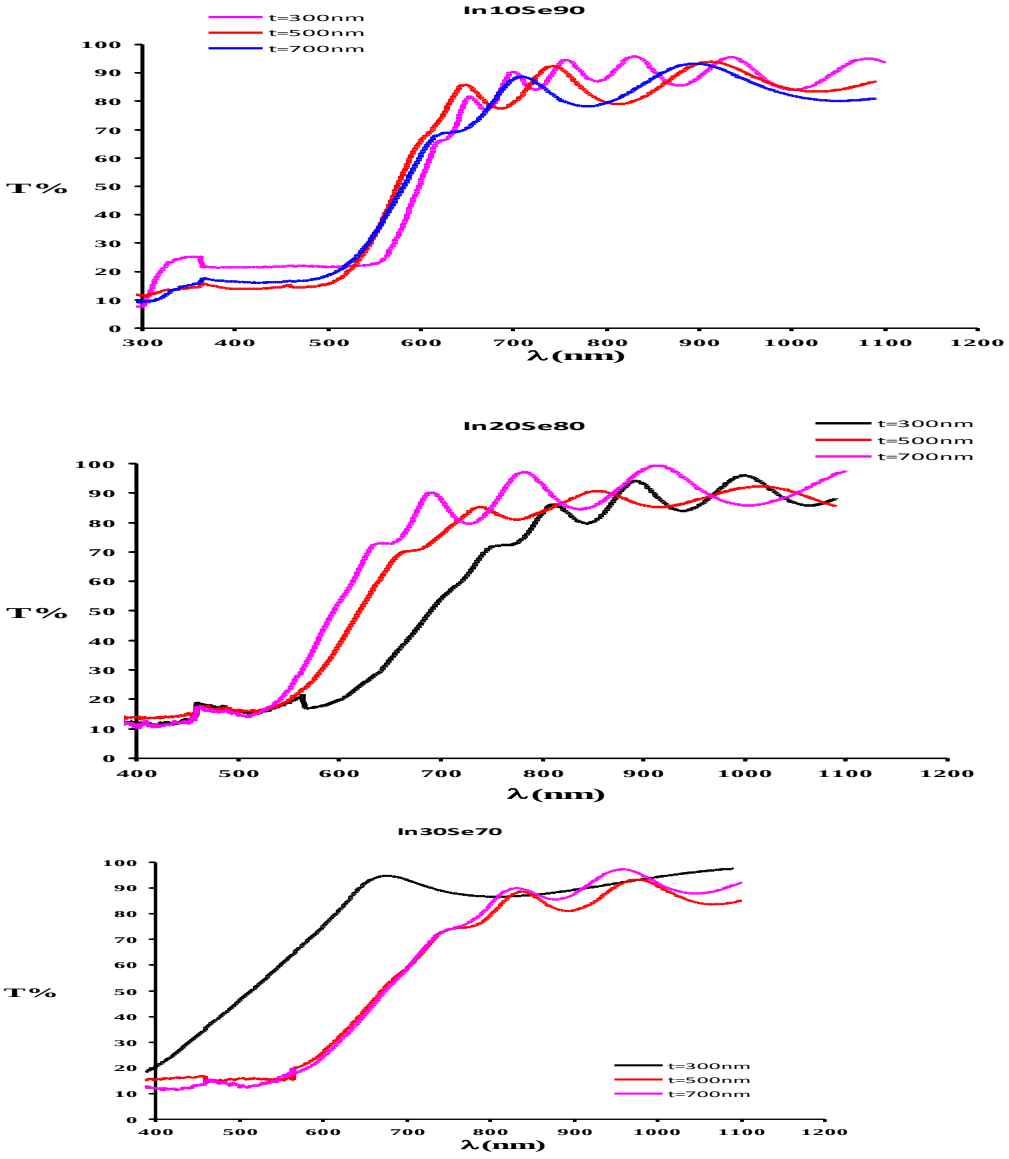

Australian Journal of Basic and Applied Sciences, 9(27) August 2015, Pages: 327-339

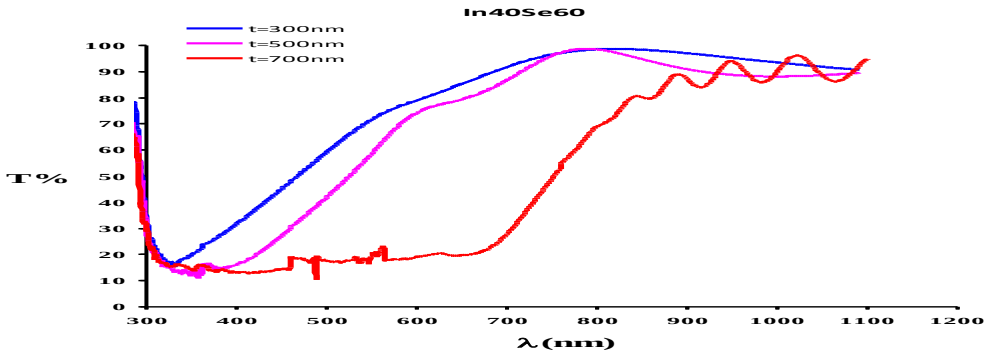

Fig. 3: The transmittance variation versus the wavelength for In_xSe_{1-x} with different In content at different thickness.

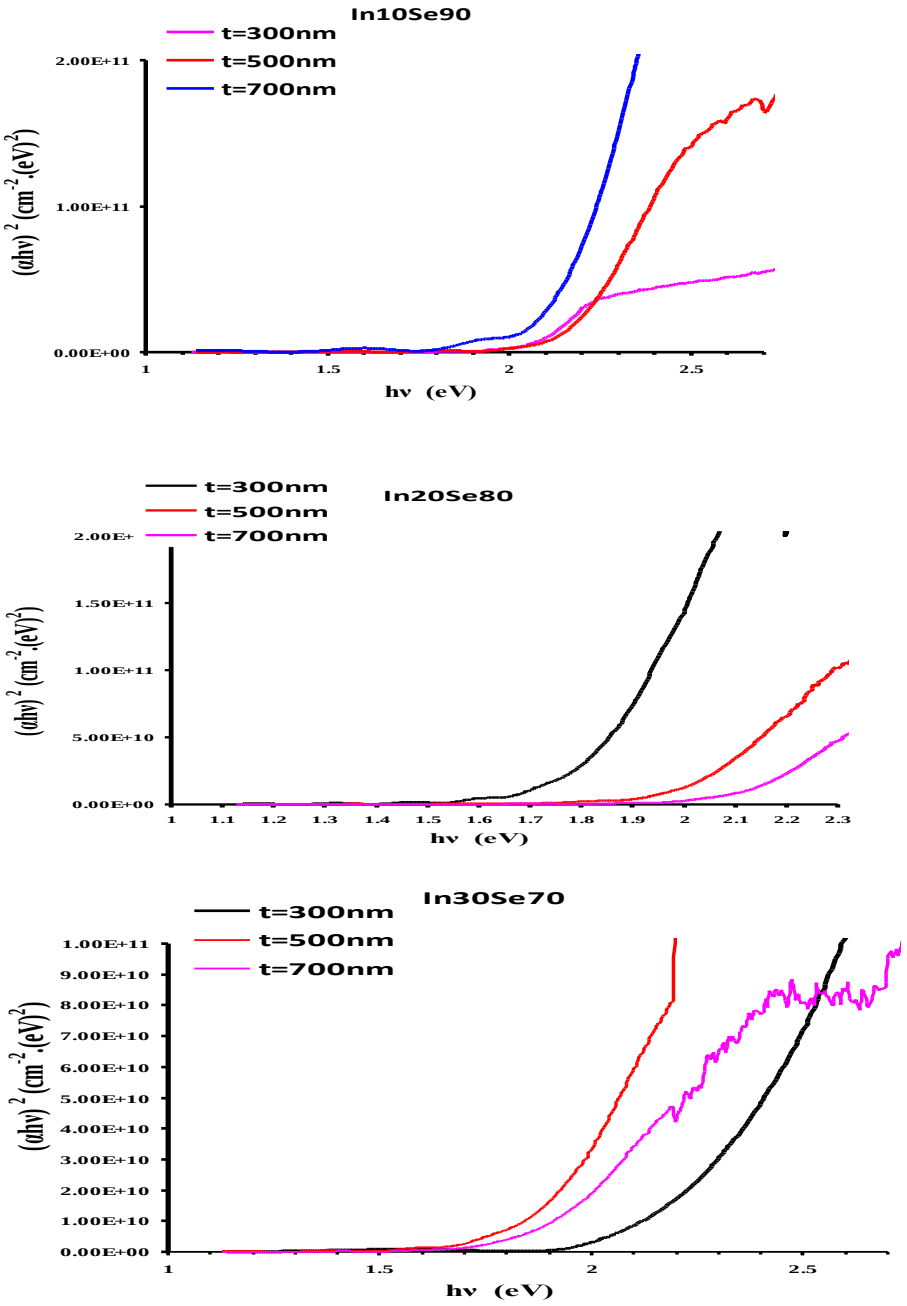

Australian Journal of Basic and Applied Sciences, 9(27) August 2015, Pages: 327-339

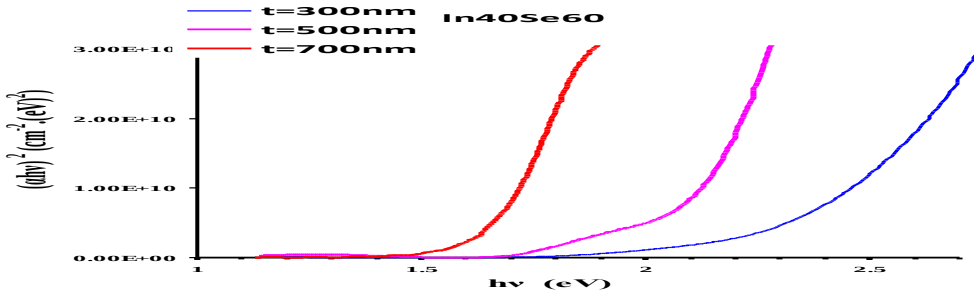

Fig. 4: Variation of$(\alpha h\upsilon)^2$ versus the photon energy ($h\upsilon$) for In_xSe_{1-x} with different In content at different thickness.

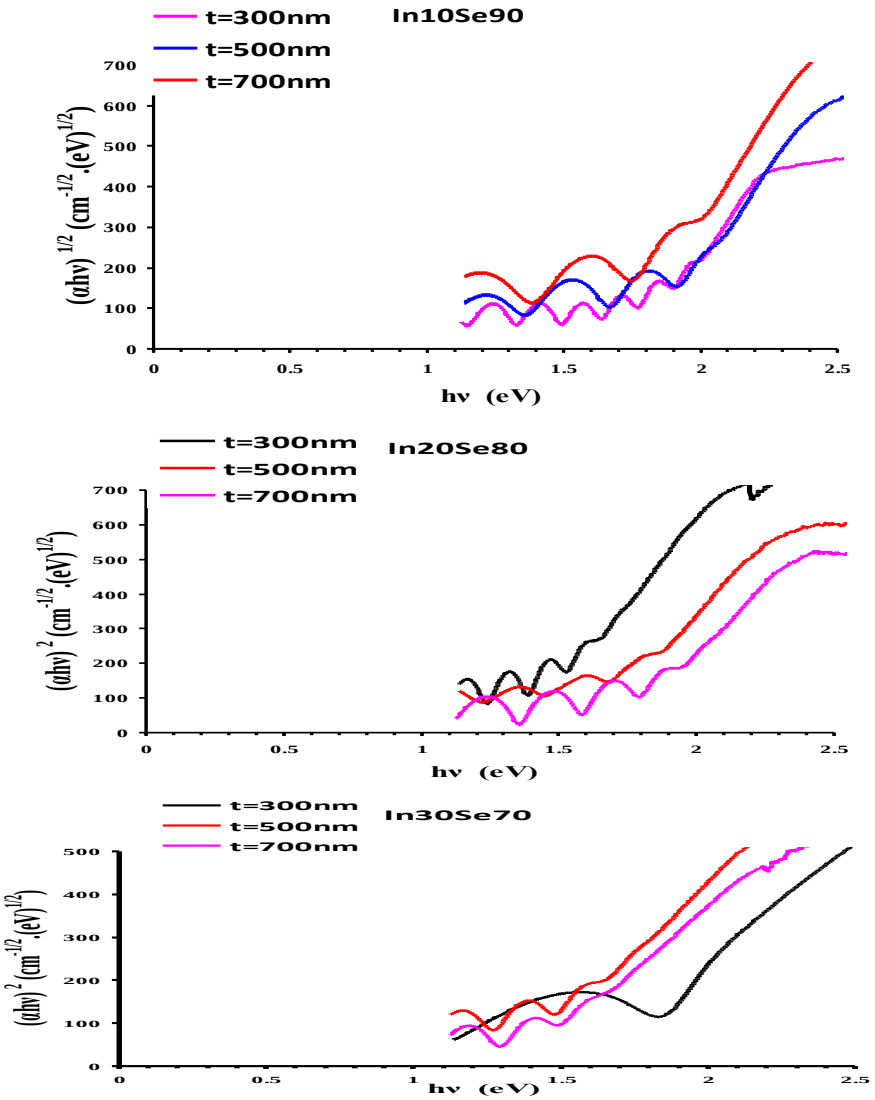

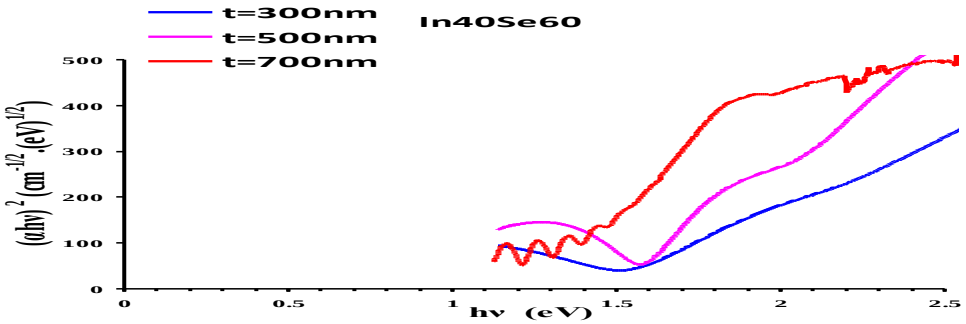

Fig. 5: Variation of$(\alpha h\upsilon)^{1/2}$ versus the photon energy (hυ)of In_xSe_{1-x} films with different thickness and different In content.

Table 3: Optical energy gap of $GeS_2)_{100-x}Ga_x$ films with different thickness and different In content.

Sample	Thickness (nm)	Direct energy gap (eV)	Indirect energy gap (eV)
$In_{10}Se_{90}$	300	2.15	1.8
	500	2.1	1.75
	700	2.05	1.74
$In_{20}Se_{80}$	300	2.1	1.7
	500	2	1.6
	700	1.8	1.45
$In_{30}Se_{70}$	300	2.2	1.58
	500	1.88	1.45
	700	1.85	1.35
$In_{40}Se_{60}$	300	2.3	1.55
	500	2.05	1.4
	700	1.65	1.3

3.4.Photoconductive Properties of In_xSe_{1-x} Films:

The photoconductivity of the In_xSe_{1-x} films has been determined with different thickness and x content at fixed intensity. The relation between dark current and the applied voltage for In_xSe_{1-x} films with different thickness and In content are shown in Fig.6 at voltage bias (0-6)V. We can observe that the current variation under illumination is relatively high for low indium content and thickness, which mean good photoconductive at low x content. While poor photoconductive is observed for high thickness and indium content ,since the dark current approach the light current , although both have high values .The incident radiation decreases the resistivity of photoconductive films by creating electronic transition in the band gap. The increase in photoconductivity is partially due to increase in the number of the free carriers (electrons and holes), and partially to decrease in the potential barrier at the grain boundaries, which increases the mobility of the carrier at the grain boundaries, and increases the photoconductivity of the carriers . We can see from this figure that the dark current increases with increasing voltage bias, at low voltage (0-4)V the increasing of dark current was small because the probability of capturing the free charge carrier by recombination and capture centers which resulting by adding In content are increased, this leading to increase the transit time (t_r)between the electrode and reduce the mobility and drift velocity. Whereas at high voltage (V>4V), when the applied electric field on the detector increased, the drift velocity is increased, for this, the defects are become un affective and this leading to reduce the transit time and the behavior of dark current was become linear as a function of high voltage bias. It is obvious at x=0.1 that dark current decreases drastically with increase of thickness, but then increases with further increase of thickness. This attributed to fill all dangling bond and vacancy which found in the structure, this leads to improve in the structure and lower the density of defect and increases the grain size (as we show in AFM pictures). Therefore the free carrier density increases and fills all the capture center, then, this centers will not effect on transfer the carrier. After that all the free charge carrier will be transfer therefore the dark current will decrease, the photocurrent increase 30 times with thickness. At x=0.2 dark current decrease with In content and increase with thickness especially at high thickness, while the photocurrent increases 85 times with increase of thickness. While at x=0.3 and 0.4 dark current increase strongly with thickness, and dark current approach photo current. This means that the sensitizing center and free charge carrier will increased as a result of In addition , then the dark current increased, whereas at low value of In content, all the effective and recombination center will filled and all the free charge carrier will transfer and extinguish, therefore the dark current decreased. The dark conductivity σ_d and photo conductivity σ_{ph} at various thickness are obtained (shown in table 5). The dark conductivity of the films increases with the thickness increasing. It should be noticed that the

conductivity is$1.55x10^{-10}(\Omega.cm)^{-1}$ to$4.88x10^{-9}$ $(\Omega.cm)^{-1}$ and from $2.34x10^{-8}$ $(\Omega.cm)^{-1}$ to $1.85x10^{-6}$ $(\Omega.cm)^{-1}$ and from $1.63x10^{-8}$ $\Omega.cm)^{-1}$ to $2.17x10^{-5}(\Omega.cm)^{-1}$and from $1.09x10^{-9}$ $\Omega.cm)^{-1}$ to $6.86x10^{-7}(\Omega.cm)^{-1}$for $In_{10}Se_{90}$ $In_{20}Se_{80}$ $In_{30}Se_{70}$ $In_{40}Se_{60}$ respectively with thickness increasing. The low conductivity of In_xSe_{1-x} films grown for low In content and thickness is due to the low grain size and the poor crystallinity of the In_xSe_{1-x} films. At high In content, the structure change from amorphous to polycrystalline. The variation of the ratio of $\Delta\sigma/\sigma$ is low for low In content i.e. x=0.1for high thickness since more photon-induced carriers will recombine because of the abundant internal defects in the films deposited at high thickness. This consequently reduces the ratio of $\Delta\sigma/\sigma$ of the films, which increases with increase of indium content and reach maximum at x=0.2 for low thickness ≤ 500 because the film has the minimum defect states which acts as recombination centers. The decreasing in $\Delta\sigma/\sigma$ as In content increases is attributed to onset of impurity conduction or increasing In concentration increase the thermal charge carriers which in turns increases the noise. The high $\Delta\sigma/\sigma$ for $In_{20}Se_{80}$ sample is due to very low dark current since it exhibit very high resistance at low temperature. The lower $\Delta\sigma/\sigma$ for $In_{30}Se_{70}$ and $In_{40}Se_{60}$ is may be ascribed to low mobility due to high concentration of impurity.

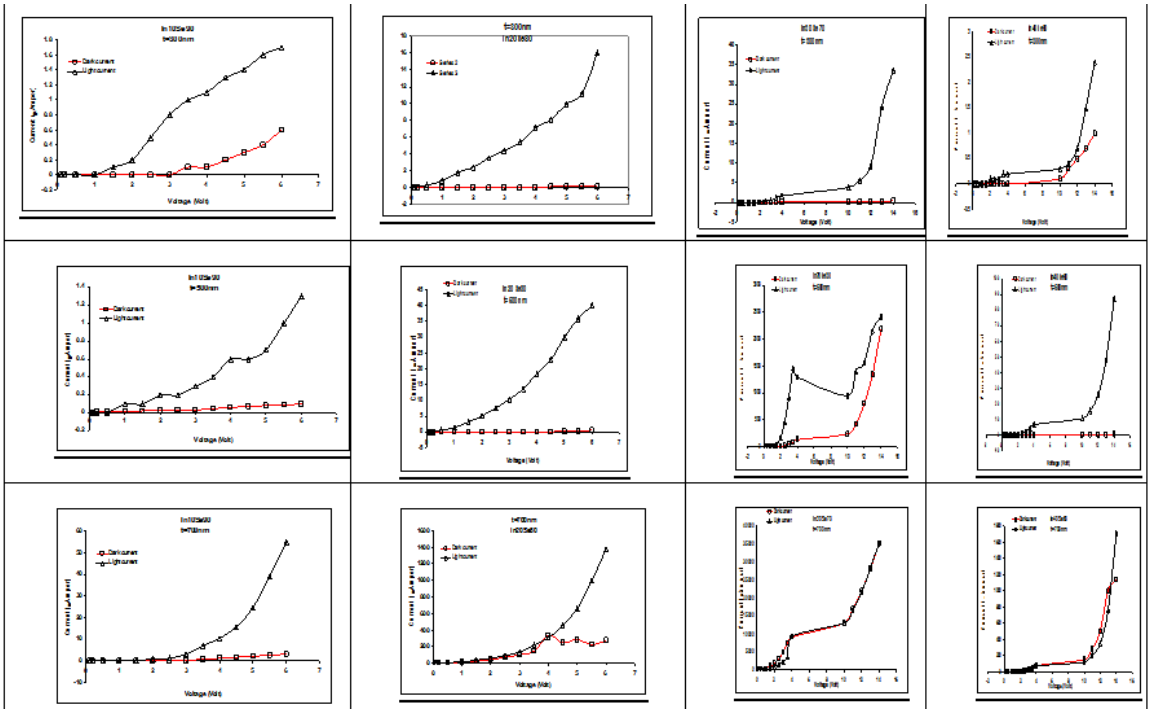

Fig. 6: The relation between dark and photocurrent and the applied voltage for In_xSe_{1-x} /n-Si PC with different thickness and In content .

Table .4 Dark-conductivity and photoconductivity of In_xSe_{1-x} thin films with different In content and different thickness.

Sample	*Thickness (nm)*	$\sigma_d(\Omega\cdot cm)^{-1}$	$\sigma_{ph}(\Omega\cdot cm)^{-1}$	$\Delta\sigma/\sigma$
$In_{10}Se_{90}$	300	1.55E-10	1.90E-09	11.24
	500	8.00E-10	3.20E-09	3
	700	4.88E-09	7.23E-08	13.82
$In_{20}Se_{80}$	300	1.87E-08	2.34E-08	123.86
	500	6.00E-08	6.65E-08	109.83
	700	5.57E-07	1.85E-06	2.32
$In_{30}Se_{70}$	300	1.96E-10	1.63E-08	82.16
	500	1.05E-06	1.40E-06	0.33
	700	2.12E-05	2.17E-05	0.02
$In_{40}Se_{60}$	300	4.72E-10	1.09E-09	1.02
	500	5.50E-10	3.93E-08	82.26
	700	5.15E-07	6.86E-07	0.33

Australian Journal of Basic and Applied Sciences, 9(27) August 2015, Pages: 327-339

3.5The Photodetector Characteristic Measurement:

From the measurements of the spectral responsivity(R_λ) for In_xSe_{1-x} films with different x content(10,20,30,and40)%and thickness(300,500,and 700nm), the spectral responsivity has been studied as shown in Fig.7 (the left side) which represent the spectral responsivity as a function of wavelength for films on n-Si substrate. It is obvious that there is almost one peak located at 600nm, this is attributed to that In_xSe_{1-x} compounds have absorption edge is observed around 580nm. The maximum value of R_λ occurs at this region relative to the incident wavelength, because the absorption of light leading to increase R_λ with increasing the wavelength incident radiation. This meaning a high efficiency to separate the electron –hole pairs which generated from the external applied field, and also to decrease the recombination processes comparing with the first region .The region beyond the absorption edge i.e. longer than 580nm R_λ reduced sharply due to approach from the wavelength cut-off (λ_c), so that the absorption decreases and the transmission increases, this means that the wavelength absorbed within the materials and this called the recombination within the materials(bulk recombination), so it has small probability for incorporate the carrier, which effect on the value of spectral response consequently the quantum efficiency decreases. From this figures the peak of R_λ are shifted to higher wavelength from 580 to 600nm with increasing In content from 10 to 20% but retain to the first location with further increase of In content as shown in Table.4 and this is attributed to increase the density of state which acts as impurities levels inside energy gap which reduced the value of E_g therefore it is shifted to higher wavelength and the films becomes more sensitive. It is clear from this table that the increasing of In content from 10 to 30% caused decrease of R_λ from 1.57 to 0.00111A/W, which due to increase of localized stated related with In addition which increases dark current and consequently reduces R_λ, however R_λ get to increase to 0.0028 A/W when In increase from 30 to 40 %this is due to results from saturation of the localized states and vacancy. Thickness has different effect on R_λ, but in general increase of thickness raised R_λ, indeed R_λ increase from 0.00111to 0.131A/W when t increases from 300to 500 nm , this behavior reflect structural enhancement (such as increase of grain size) with increase of thickness as see from AFM measurement.

The quantum efficiency (η) values are related to spectral response results it was calculated. Fig.7 (the middle) shows the variation of η versus wavelength of In_xSe_{1-x} films with different x content (10,20,30 and 40) and thickness(300,500,and 700nm). It can be seen from the Table. 6 and Fig.8 that the η decreases sharply with increase of In content but then increase with further increase of In. Indeed η decrease from 33.6 % to 0.23% when In increase from 10 to 30, but η increases to 0.59 % with increase of In to 40 . This is attributed to the decrease of R_λ with increasing In content, also increasing of In content increase reflectance on the expense of absorbance with lead to decrease quantum efficiency.

The specific detectivity(D^*) can be defined as the minimum incident power falling on the detector can be detected by the detector and it represent one of the main parameters which is the criteria for the suitable application for the detectors. The values of D* were calculated from the measured values of R_λ an I_N (the total noise current) for In_xSe_{1-x} films with different x content (10,20,30 and 40)% and thickness (300,500,and 700nm)and plotted in Figs.9(in the right). It is seen from these figures that the higher magnitude of D^* proportional with the higher magnitude of the R_λ because the D^* is a function of the spectral response. Also the D^* decrease about three order of magnitude with increase of In content. Indeed D^* decreases from 1.5 $x10^{12}$ to 5.5 $x10^9$ $cmHz^{1/2}.W^{-1}$ when In increases from 10 to 40. while thickness has different effect on D^* values . D* decrease with thickness for In content 10and 30 while D* increases with thickness for In content 20 and 40 .It is found that the detectivity of photoconductive device is markedly dependent on the deposition technique, and the detectivity increases at low temperature and its peak shifts to longer wavelength. As we expected the performance of In_xSe_{1-x} fabricated detector is high for the lower $\Delta\sigma/\sigma$ and associated noise at x=0.1 while the poor performance for samples of residual In content with high thickness . This refereed that maximum D* value or maximum detectable is obtained for $In_{10}Se_{90}$ detector corresponding to minimum $\Delta\sigma/\sigma$. while minimum D* value or maximum detectable is obtained for $In_{20}Se_{80}$ detector corresponding to maximum $\Delta\sigma/\sigma$. It is found that for optimum photoconductivity gain $\Delta\sigma/\sigma$, the minimum detectable power will be lowered as compared to the case without gain. If the gain exceeded the optimum value the sensitivity decreases more because of excess noise associated with carrier multiplication.

Table 5: R(λ), η% and D* of In_xSe_{1-x} thin films with different In content and different thickness at λ=600nm.

Sample	Thickness (nm)	R(λ)(A/W)	η%	D*(cm.Hz$^{1/2}$)/W
$In_{10}Se_{90}$	300	1.57	33.67	$1.5X10^{12}$
	500	0.266	12.8	$1.98X10^{13}$
	700	0.06	57.01	$1.29X10^{12}$
$In_{20}Se_{80}$	300	0.00371	0.767	$3.7X10^{9}$
	500	$0.0037X10^{-3}$	0.00076	$1.9X10^{9}$
	700	0.0076	1.63	$1.8X10^{11}$
$In_{30}Se_{70}$	300	0.0011	28.14	$9.99X10^{9}$
	500	0.0485	10.36	$1.27X10^{12}$
	700	0.131	0.238	$4.6X10^{10}$
$In_{40}Se_{60}$	300	0.0028	0.59	$5.4X10^{9}$
	500	0.11	23.5	$4.7X10^{9}$
	700	0.174	37.37	$3.4X10^{12}$

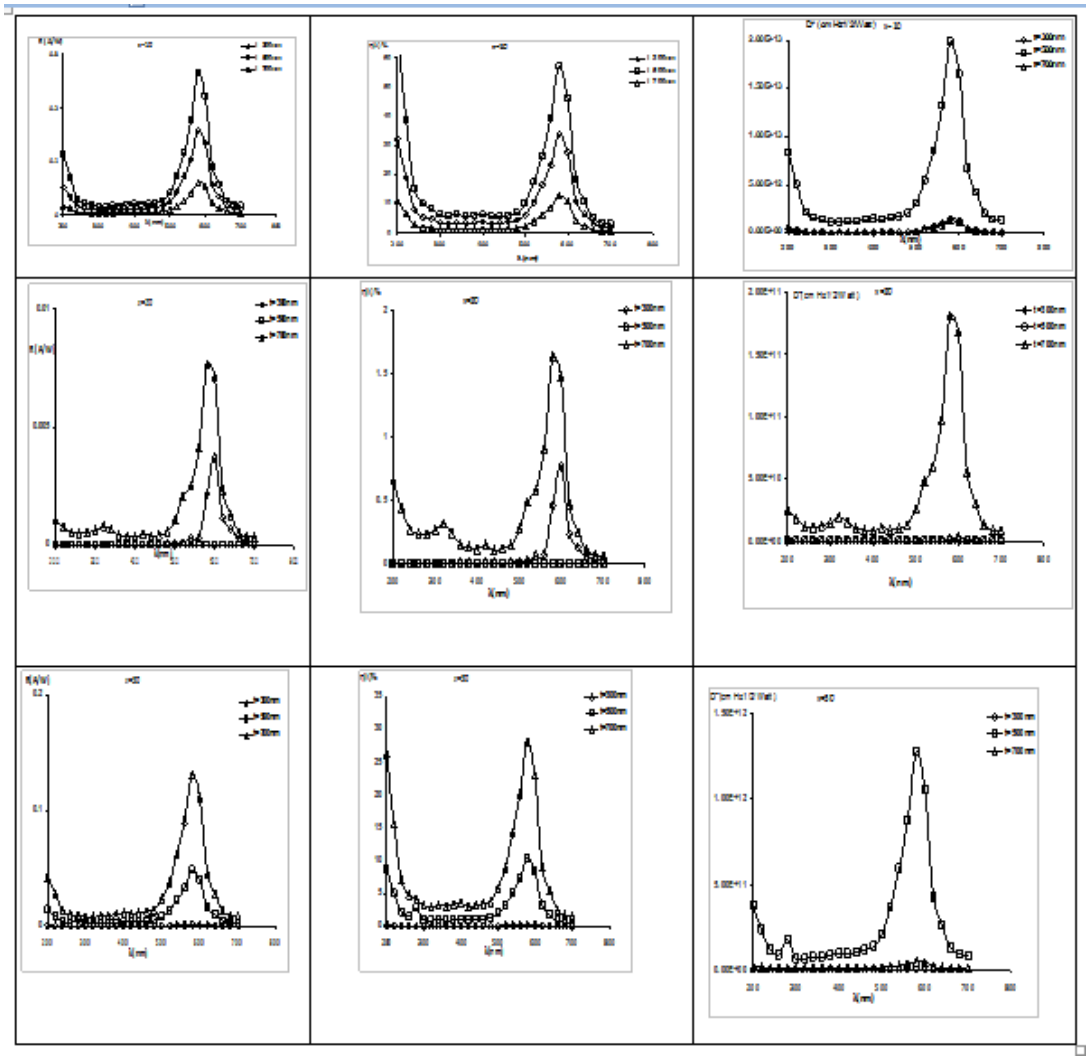

Fig. 7: (the left side)Responsivity versus wavelength of for PC In_xSe_{1-x} with different thickness and In content .
Fig. 8: (the middle)quantum efficiency versus wavelength of for PC In_xSe_{1-x} with different thickness and In content.
Fig. 9: (the right side)detectivity versus wavelength of for PC In_xSe_{1-x} with different thickness and In content .

Conclusions:

From the data of the present work, we can conclude that

1- The In_xSe_{1-x} alloys for (x = 0.1, 0.2, 0.3, 0.4) have successfully prepared, which was used for bulks and films preparation at different conditions.

2. From AFM and EDAX studies, we are determined the concentration of In content for these alloys, and the result are of high accuracy and very close to the theoretical values.

3. Increasing of In and thickness made In_xSe_{1-x} thin films more opaque to the incident radiation.

4. In_xSe_{1-x} thin films revealed direct and indirect transition.

5. $In_{10}Se_{90}$ and $In_{20}Se_{80}$ thin films are the most promise for photodetector .

6- In_xSe_{1-x} samples are visible - infrared photoconductors with response to about 600nm. An enhancement in the performance (i.e. the high spectral detectivity values) can be obtained with low indium concentration which leads to low noise or high dark resistance.

REFERENCES

Di Giulio, M., G. Micocci, R. Rella, P. Siciliano and A. Tepore, 1987. Thin Solid Films, 148: 273-278.

El-Zahed, H., A. El-Korashy and M. Abdel Rahman, 2002. 68: 19.

El-Zahed, H., A. El-Korashy, M. Abdel Rahman, 2003. Effect of heat treatment on some of the optical parameters of Cu9Ge11Te80 films, 68: 19-27.

Emery, J.Y., L. Brahim-Otsmane, M. Jouanne, C. Julien and M. Balkanski, 1989. Materials Science and Engineering B 3: 13-17.

Gopal, S., C. Viswanathan, B. Karunagara, Sa. K. Narayandass, D

Grigorov, S.N., V.M. Kosevich, S.M. Kosmachev, A.V. Taran, 2004. Physics and Chemistry of Solid State., 5: 35-37.

Grigorov, S.N., V.M. Kosevich, S.M. Kosmachev, A.V. Taran, 2004. Physics and Chemistry of Solid State., 5: 35-37.

Hasegawa, Y., Y. Abe, 1982. Phys. Stat. Sol. A79,615.

Krus, P.W., 1977.“ Optical and Infrared Detectors ”, ed. R.J.Keyes Springer-Verlag Berlin , Heidelberg, 19.

Mott, N.F. and E.A. Davis, 1979. Electronic Process in non-crystalline materials, 2nd Edn, Clarendon Press, Oxford.

Mutlu, I.H., M.Z. Zarbaliyevand F.Aslan, 2007. J. of Sol-Gel Science and Technology, 43: 223-226.

Pankove, J.I., 1971. Optical Processes in Semiconductors, New Jersey: Prentice-Hall, p: 93.

Parlak, M. and Ç. Erçelebi, 1998. Thin Solid Films., 322: 334-339.

Peršin, M., A. Peršin, B. Čelustka, 2005. Thin Solid Films 12: 117-122 (1972). International Journal of Renewable Energy Technology Research Vol. 2, No. 9, September 2013, PP: 220 - 226, ISSN: 2325-3924 (Online) Available online at http://ijretr.org 226 Technol., 40: 557-562.

Peršin, M., B. Čelustka, B. Markovič and A. Peršin, 1970. Thin Solid Films 5: 123-128.

Qasrawi, A.F., 2007. Optical Materials, 29: 1751-1755.

Qasrawi, A.F., 2007. Temperature dependence of the band gap,refractive index and single-oscillator parameters of amorphous indium selenide thin films, Optical Materials, 29: 1751-1755.

Rusu, G.G., 2001. J. of Optoelectronics and Advanced Materials, 3: 861.

Rusu, G.G., 2001. J. of Optoelectronics and Advanced Materials, 3: 861.

Samuel Lioo, Y., 1984. ”Microwave Solid State Devices”.

Savitskii, A.V., M.V. Kurik, K.D. Tovstyuk, 1964. Opt.Spectrose., 19: 56.

Tauc, J., 1974. Amorphous and Liquid Semiconductors, NewYork: Plenum Press, Chap: 4.

Tolansky, S., 1948. Multiple beam interferometry of surface and films, Oxford University Press, London.

Viswanathan, C., G. G. Rusu, S. Gopal, D.Mangalaraj, Sa. K. Narayandass, 2005. J. of Optoelectronics and Advanced Materials, 7: 705-711.

Viswanathan, C., G.G. Rusu, S. Gopal, D. Mangalaraj, S.K.Narayandass, 2005. On the electrical characteristics of vacuum evaporated indium selenide thin films, J. Optoelectronics and Advanced Materials., 7: 705-711.

Viswanathan, C., G.G. Rusu, S. Gopal, D. Mangalaraj, Sa. K. Narayandass, 2005. J. of Optoelectronics and Advanced Materials, 7: 705-711.

Viswanathan, C., G.G. Rusu, S. Gopal, D. Mangalaraj, Sa. K. Narayandass, 2005. J. of Optoelectronics and Advanced Materials, 7: 705-711.

Viswanathan, C., G.G. Rusu, S. Gopal, D.Mangalaraj, Sa. K. Narayandass, 2005. J. of Optoelectronics and Advanced Materials, 7: 705-711.

Viswanathan, C., G.G. Rusu, S. Gopal, D.Mangalaraj, Sa. K. Narayandass, 2005. J. of Optoelectronics and Advanced Materials, 7: 705-711.

Viswanathan, C., V. Senthilkumar, R. Sriranjini, D. Mangalaraj, Sa. K. Narayandass, 2004. Junsin Yi, Crystal Research and Tech, 40: 658-664.

Viswanathan, C., V. Senthilkumar, R. Sriranjini, D.Mangalaraj, S.K. Narayandass, J.S. Yi, 2004. Effect of substrate temperature on the properties of vacuum evaporated indium selenide thin films, Crystal Research and Tech, 40: 658-664.